VNU Journal of Science: Mathematics - Physics

Journal homepage: https://js.vnu.edu.vn/MaP

Original Article

Synthesis of V_2O_5-SnO_2 Nanocomposite for NH_3 Detection at Low Temperature

Bui Thanh Hung[1,2], Dang Thi Thanh Le[1,2], Nguyen Duc Hoa[1,2], Nguyen Van Duy[1,2], Nguyen Pham Yen Nhi[1,2], Chu Manh Hung[1,2,*]

[1]*Faculty of Electronic Materials and Devices, School of Materials Science and Engineering (SMSE), Hanoi University of Science and Technology (HUST), 1 Dai Co Viet, Hanoi, Vietnam*

[2]*International Training Institute for Materials Science (ITIMS), Hanoi University of Science and Technology (HUST), 1 Dai Co Viet, Hanoi, Vietnam*

Received 7th August 2025
Revised 4th October 2025; Accepted 29th December 2025

Abstract: The V_2O_5-SnO_2 nanocomposite was synthesized through a combination of hydrothermal synthesis and subsequent mechanical mixing. Gas-sensing properties of the synthesized nanocomposite were investigated. The results demonstrated that the nanocomposite sensor exhibited notable sensitivity toward ammonia (NH_3) at a low operating temperature of 50 °C. Specifically, the sensor achieved a response of 2.3 at an NH_3 concentration of 1000 ppm. At this temperature, the V_2O_5-SnO_2-based sensor also displayed good selectivity and repeatability toward NH_3, indicating its potential for reliable low-temperature gas sensing applications..

Keywords: V_2O_5-SnO_2, nanocomposite, hydrothermal, NH_3, gas sensor.

1. Introduction

Gas sensors based on metal oxides have been extensively studied worldwide due to their high response, good portability and low fabrication cost. However, as well known, working temperature largely determines the gas sensing performance, which controls the reaction kinetics, conductivity and electron mobility [1]. Furthermore, high working temperature operation signifies energy waste, which adversely limits its wide application. Therefore, semiconductor working at low-temperature is a trend and necessity.

* Corresponding author.
E-mail address: hung.chumanh@hust.edu.vn

https//doi.org/10.25073/2588-1124/vnumap.5058

Vanadium pentoxide (V_2O_5), a transition metal oxide with a characteristic layered structure and variable electronic properties, has garnered significant interest for gas sensing applications [2]. Vanadium exhibits an electron configuration of [Ar] $4s^23d^3$ and can adopt multiple oxidation states, ranging from −3 to +5, with +5, +4, +3, and +2 being the most prevalent. Various vanadium oxides corresponding to these oxidation states have been reported, including VO (+2), VO_2 (+4), V_2O_3 (+3), V_2O_5 (+5), and mixed-valence oxides such as V_3O_7, V_4O_9, and V_6O_{13} [3]. Due to its p-type semiconducting nature, redox flexibility, and layered morphology, V_2O_5 demonstrates strong potential for detecting reducing gases such as NH_3, H_2S, and CO [4].

Tin dioxide (SnO_2) is a widely studied n-type semiconductor with a wide band gap of approximately 3.6 eV at room temperature [5]. Its electrical conductivity predominantly arises from intrinsic defects, particularly oxygen vacancies, which act as donor sites providing free electrons. Owing to its high electrical conductivity, pronounced surface reactivity, excellent thermal stability, and the ability to be synthesized in diverse nanostructured morphologies, SnO_2 is considered a leading material for gas sensing applications. It has demonstrated high sensitivity toward a variety of toxic and flammable gases, including ammonia (NH_3), carbon monoxide (CO), hydrogen (H_2), nitrogen dioxide (NO_2), and various volatile organic compounds (VOCs) [6-8].

V_2O_5/SnO_2 composites represent a class of semiconductor oxide heterojunction systems that have attracted considerable interest in gas sensing due to the synergistic integration of their individual advantages. SnO_2, a widely studied n-type semiconductor, is known for its high electrical conductivity and excellent thermal stability, while V_2O_5, a transition metal oxide, exhibits strong surface catalytic activity and efficient electron exchange due to its multiple accessible oxidation states [4]. Depending on the synthesis conditions and the oxidation state of vanadium, the V_2O_5/SnO_2 system can form either n–n or p–n heterojunctions, which enhance the interfacial barrier potential and promote efficient charge separation and transfer during interaction with target gases. Numerous studies have demonstrated that V_2O_5/SnO_2 composites exhibit improved sensitivity, selectivity, and low-temperature sensing performance compared to their individual components [9-11].

In this study, V_2O_5-SnO_2 was synthesized by hydrothermal method followed by mechanical mixing, and their properties were characterized using scanning electron microscopy (FESEM), X-ray diffraction (XRD). The gas-sensing performance of the prepared V_2O_5-SnO_2 material towards ammonia at working temperature of 50 ^oC was evaluated and the sensor exhibited good response to ammonia gas.

2. Experimental

Ethylene glycol, NH_4VO_3, $SnCl_4.5H_2O$, Pluronic P123, oxalic acid, ethanol, acetone, N-Vinylpyrrolidone (NVP), HNO_3, NaOH, were all used as received without further purification.

First, a total of 1.17 g of ammonium metavanadate (NH_4VO_3) was dissolved in a mixed solvent comprising 30 mL of ethylene glycol and 30 mL of deionized water under continuous stirring at room temperature for 15 minutes. Subsequently, 1 g of Pluronic P123 was added to the solution and stirred for an additional 30 minutes until fully dissolved. Oxalic acid (10 mmol) was then gradually introduced into the mixture with continuous stirring for approximately 15 minutes, resulting in a pH reduction to ~4. The resulting solution was transferred into a Teflon-lined autoclave and subjected to hydrothermal treatment at 200 °C for 24 hours. The obtained product was filtered, washed with deionized water three times, and dried. Finally, the dried sample was calcined in air at 500 °C for 2 hours to yield the desired powder.

Parallelly, tin (IV) chloride pentahydrate ($SnCl_4 \cdot 5H_2O$, 0.9 g) was dissolved in a mixed solvent of 20 mL deionized water and 20 mL ethanol under continuous stirring for 10 minutes. Subsequently, 0.8 g of sodium hydroxide (NaOH) was added to the solution and stirred for an additional 30 minutes.

Following this, 0.04 g of nitric acid (HNO_3) was introduced, and the mixture was stirred for a further 30 minutes to ensure complete reaction. The resulting solution was transferred to a Teflon-lined autoclave and subjected to hydrothermal treatment at 160 °C for 24 hours. After cooling, the solid product was collected by filtration, washed thoroughly with deionized water three times, and dried. The obtained powder was then calcined in air at 500 °C for 2 hours.

Following the successful hydrothermal synthesis of individual V_2O_5 and SnO_2 nanomaterials, the V_2O_5/SnO_2 composite was prepared via mechanical mixing in an N-vinylpyrrolidone (NVP) solution with the weight ratio of 1:1. The sensor is named as SV11. This approach facilitates uniform dispersion of the nanoparticles and promotes interfacial interactions between the two components, thereby enhancing the miscibility and structural homogeneity of the resulting composite material. The whole procedure is shown in Fig. 1.

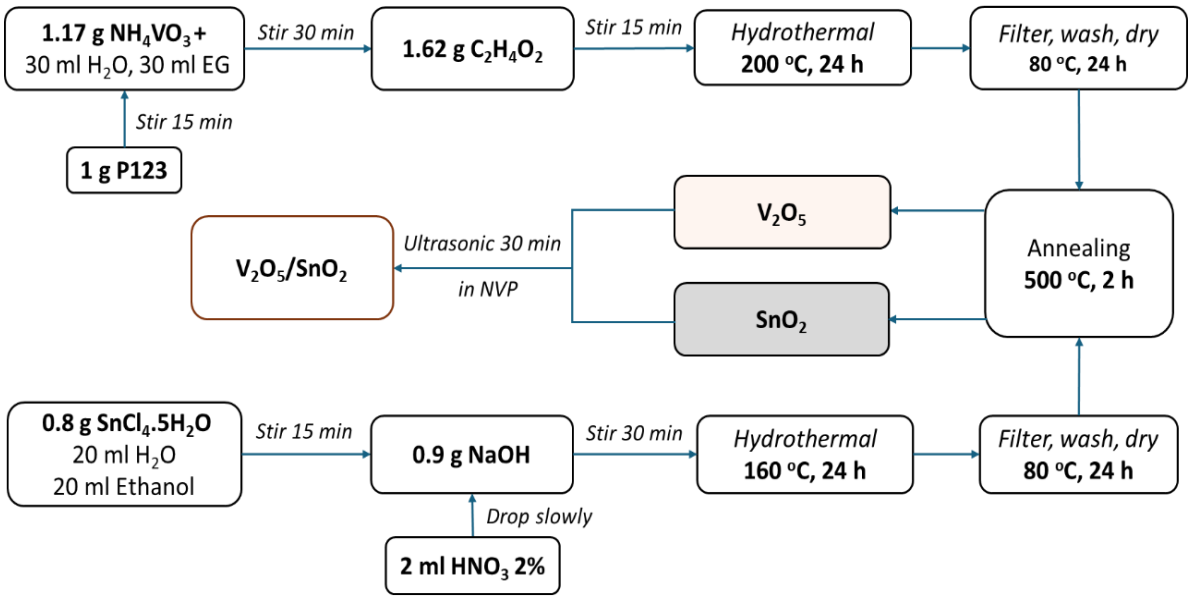

Figure 1. Preparation procedure of V_2O_5-SnO_2 nanocomposites.

The annealed nanomaterials were characterized and analyzed by using X-ray diffraction (XRD), and scanning electron microscopy (SEM). The XRD analysis was performed using a Bruker D5005 X-ray diffractometer with CuKα1 radiation (λ = 1.5406 Å) at 40 kV and 40 mA. SEM images were obtained using a JEOL7600 scanning electron microscope at an accelerating voltage of 20 kV.

The as-synthesized nanocomposite was deposited via electrospinning onto Si/SiO_2 substrates bearing interdigitated Pt electrodes, yielding a uniform, mechanically robust sensing film. The electrode assemblies were subsequently annealed in ambient air at 500 °C for 2 h to improve film stability and interfacial adhesion. Electrical resistance measurements were performed using a Keithley 2602 source meter while the sensor was subjected to cyclic exposures of NH_3 in dry air. Gas concentrations (50–1000 ppm) were precisely metered using MKS GV50 mass flow controllers, with a constant total flow rate of 400 sccm. All gas-sensing tests were carried out at 50 °C in a bespoke measurement chamber. Sensor response was defined as $S = R_g/R_a$ where R_a and R_g denote the steady-state resistances in air and in the presence of the target gas, respectively [12, 13].

3. Results and Discussion

3.1. Nanocomposite Characterization

Scanning electron microscopy (SEM) analysis of V_2O_5 reveals the formation of highly porous, spherical architectures resembling nanoflowers or urchin-like structures. At low magnification as shown in Fig. 2A, these flower-like morphologies, with average diameters ranging from approximately 5 to 10 µm, are uniformly distributed across the sample surface. Higher-magnification images show that each structure consists of ultrathin, radially oriented nanosheets emanating from a central core (Fig. 2B). This hierarchical and porous morphology indicates a high specific surface area and an open pore network, both of which are advantageous for enhancing gas adsorption and diffusion—key factors in the performance of gas sensors.

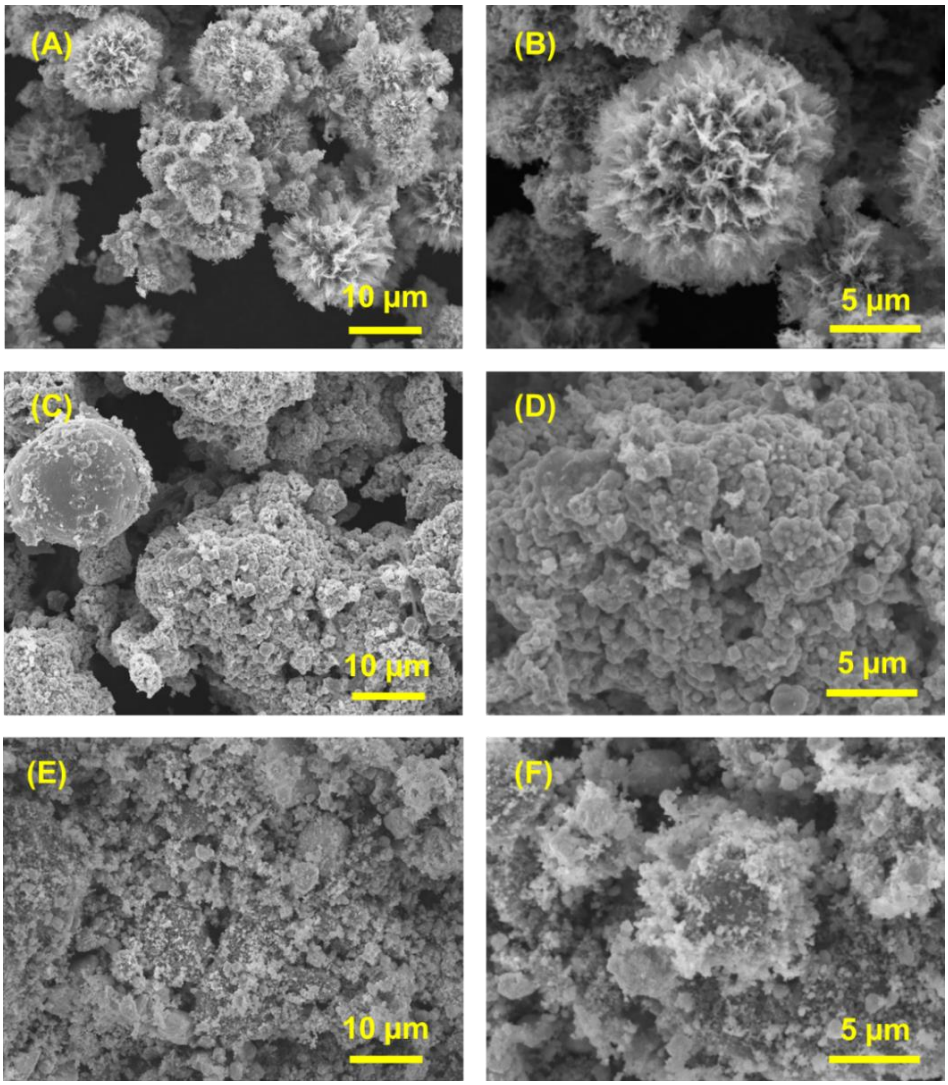

Figure 2. SEM images of (A, B) V_2O_5, (C, D) SnO_2 and (E, F) V_2O_5-SnO_2 nanocomposite at diverse magnifications.

SEM images of SnO_2 samples, as shown in Fig. 2C and Fig. 2D, reveal a spherical granular morphology with particle sizes ranging from approximately 20 to 50 nm. However, these nanoparticles are not well-isolated; instead, they exhibit a strong tendency to aggregate, forming larger clusters.

Following mechanical mixing, the material exhibited an agglomerated morphology with a non-uniform micrometer-scale distribution as shown in Fig. 2E, F. Notably, several large, porous spherical structures with diameters of approximately 2-4 μm were observed, likely originating from V_2O_5 clusters formed by the self-assembly of nanosheets during synthesis. Despite mechanical grinding using a mortar and subsequent ultrasonic treatment, these flower-like architectures were partially retained, indicating a relatively stable interconnection among the nanostructured units.

Surface analysis also revealed the presence of smaller nanoparticles—presumed to be SnO_2—either adhered to or dispersed around the V_2O_5 structures. However, due to the limited dispersion efficiency of the mechanical mixing process, large agglomerates remained, potentially compromising the uniformity and reducing the effective surface area of the composite material.

X-ray diffraction (XRD) analysis of the mechanically mixed V_2O_5 and SnO_2 powders confirms that the characteristic diffraction patterns of both components are preserved. The observed diffraction peaks correspond well with the standard reference patterns for V_2O_5 (ICDD No. 01-089-0612) and SnO_2 (ICDD No. 01-077-0451), with no additional peaks or shifts indicative of new phases or chemical reactions. This suggests that the mixing process involves only a physical combination of the two materials without the formation of any secondary phases or compound structures. Consequently, the properties observed in the resulting composite can be attributed to the inherent characteristics of the V_2O_5-SnO_2 nanocomposite, unaffected by impurity phases or structural transformations during fabrication.

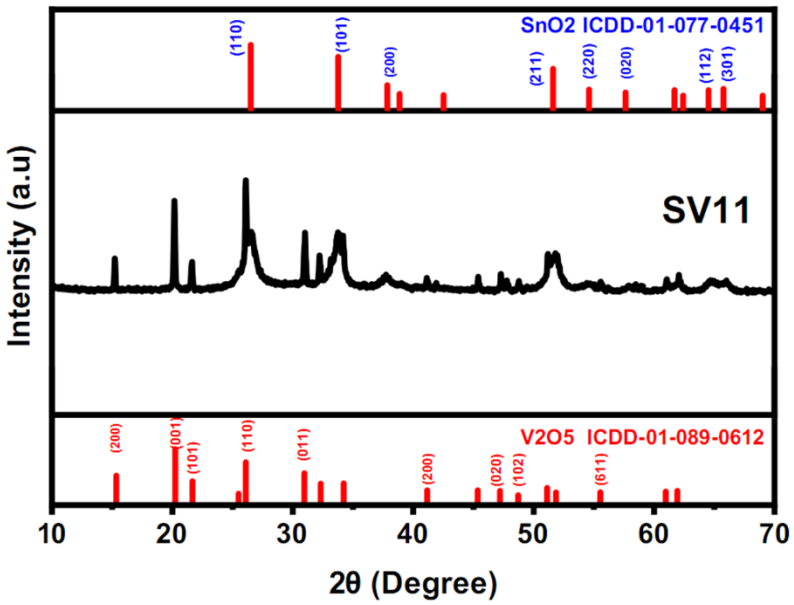

Figure. 3. XRD pattern of V_2O_5-SnO_2 nanocomposites.

3.2. Gas Sensing Property

For ammonia sensing investigations, V_2O_5-SnO_2 nanocomposites were selected as the sensing material. The time-dependent response alterations of the WO_3 sensor were surveyed while operating at

various operating temperatures and subjected to varying concentrations of NH_3 gas (50, 125, 250, 500 and 1000 ppm). The results, illustrated in Fig. 4A, furnish valuable insights into the gas sensitivity of V_2O_5-SnO_2 nanocomposites towards NH_3.

Fig. 4A illustrates five real-time response profiles of the V_2O_5-SnO_2 nanocomposite sensor while operating at temperature of 50 °C. Upon exposure to NH_3 gas, the sensor exhibited an increase in resistance, subsequently reverting to its initial state upon the removal of the gas source. This behavior is indicative of the p-type semiconductor characteristics inherent to the V_2O_5-SnO_2 nanocomposites.

Fig. 4B presents the response data derived from Fig. 4A. These results underline that at the operational temperature of 50 °C, the WO_3 sensor demonstrated its highest sensitivity when exposed to 1000 ppm NH_3 gas, exhibiting a response value (S) of 2.2. For NH_3 concentrations of 50, 125, 250, 500 and 1000 ppm, the response values were 1.1, 1.2, 1.3, 1.5 and 2.3, respectively. It is noteworthy that the sensor's response exhibited a linear trend with increasing gas concentration.

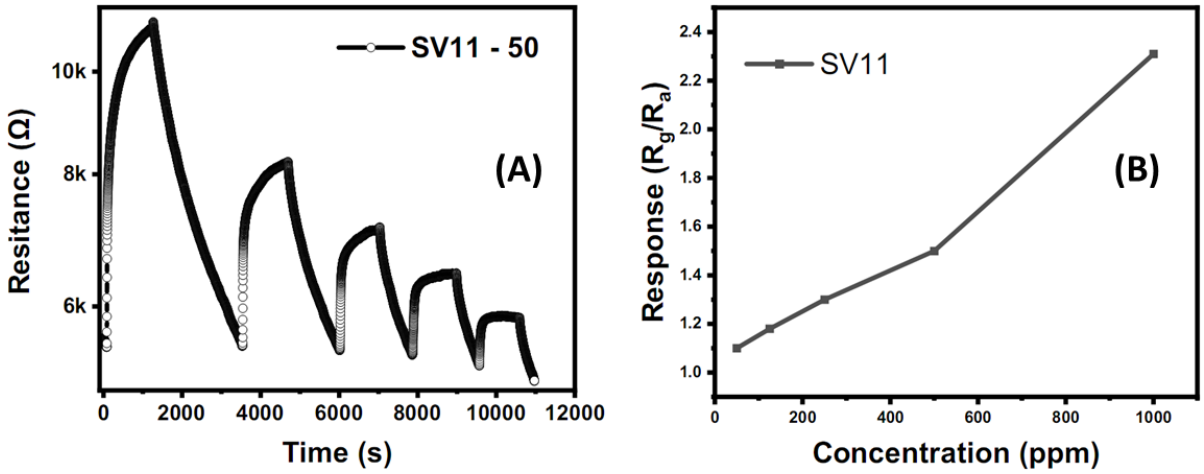

Figure 4. The response of the V_2O_5-SnO_2 sensor to NH_3 gas at 50 °C: (a) Transient response as a function of time various concentrations from 25 to 500 ppm at 50 °C, (b) Response behavior as a function of concentration at 50 °C.

V_2O_5-SnO_2 nanocomposite shows p-type semiconductor characteristic at working temperature of 50°C. When V_2O_5-SnO_2 nanocomposite is exposed to ambient air, oxygen molecules have a tendency to adsorb onto their surface, adopting the form of O_2^- ions as the following equation (1):

$$O_2 + e^- \rightarrow O_2^- \quad (1)$$

This phenomenon results in a significant accumulation of adsorbed oxygen ions on the sensor surface, which extract electrons from the semiconductor, leading to electron depletion within the nanostructure. Upon exposure to ammonia, the NH_3 molecules undergo surface reactions with these adsorbed oxygen species, as represented by the reaction (2) below:

$$2NH_3 + 3/2O_2^- \rightarrow N_2 + 3H_2O + 3/2e^- \quad (2)$$

This interaction leads to the release of previously trapped electrons, allowing them to return to the nanocomposite material. As a result, the hole concentration within the nanocomposite decreases, causing a corresponding increase in the sensor's electrical resistance.

The SV11 sensor demonstrated a stable and reproducible response when exposed to 1000 ppm of NH_3 over eight consecutive measurement cycles at 50 °C as show in Fig. 5A. The amplitude of resistance variation remained nearly constant across all cycles, indicating excellent signal stability and consistent

performance. These results suggest that the sensor possesses good reliability and repeatability for NH_3 detection under the tested conditions.

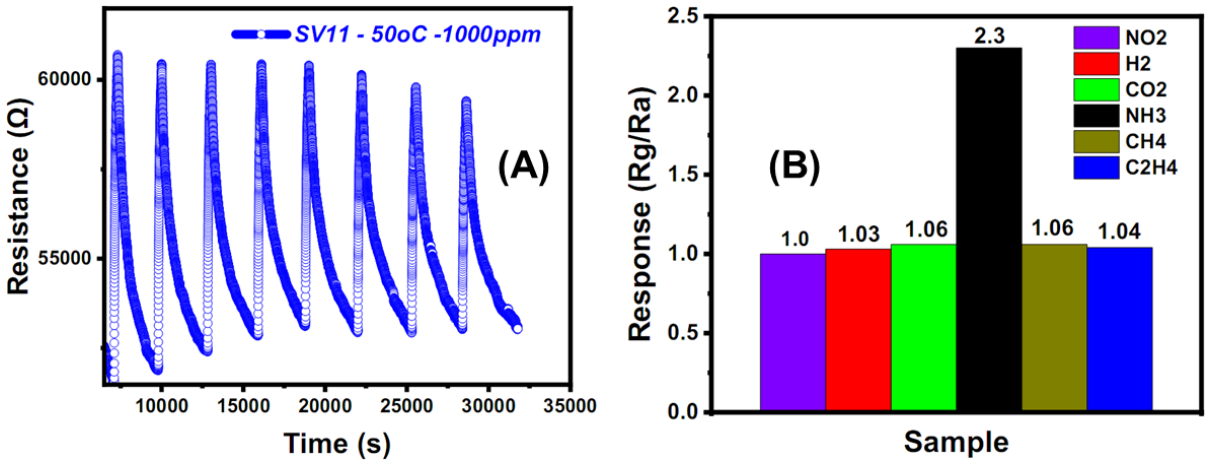

Figure 5. (A) The repeatability of the V_2O_5-SnO_2 sensor to NH_3 at 50 °C, (B) The selectivity of the V_2O_5-SnO_2 sensor to various gases at 50 °C.

In NH_3 gas sensing applications, selectivity-the ability to differentiate the target gas from other interfering species-is a critical parameter, particularly in environments where chemically similar gases coexist. To assess this, the sensor was evaluated against several common gases, including H_2, NO_2, CO_2, CH_4, and C_2H_4, at 50 °C. As illustrated in Fig. 5B, the sensor exhibited a pronounced response to NH_3, while the responses to the other gases were negligible, demonstrating good selectivity toward NH_3 under the tested conditions.

4. Conclusion

In this study, a V_2O_5-SnO_2 nanocomposite was synthesized via a hydrothermal method followed by mechanical mixing. Structural characterization revealed that the composite possessed a porous morphology. The ammonia sensing performance of the material was subsequently evaluated, and the sensor exhibited a notable response of 2.3 to 1000 ppm NH_3 at an operating temperature of 50°C. These results confirm the successful fabrication of the V_2O_5-SnO_2 nanocomposite and underscore its potential for low-temperature NH_3 sensing applications.

Acknowledgments

This research is funded by the Ministry of Science and Technology of Vietnam under Grant No. ĐTĐL.CN-35/23.

References

[1] Z. Li, H. Li, Z. Wu, M. Wang, J. Luo, H. Torun, P. Hu, C. Yang, M. Grundmann, X. Liu, Y. Fu, Advances in Designs and Mechanisms of Semiconducting Metal Oxide Nanostructures for High-precision Gas Sensors Operated at Room Temperature, Materials Horizons, Vol. 6, 2019, pp. 47-506, https//doi.org/10.1039/c8mh01365a.

[2] S. Rani, M. Kumar, P. Garg, R. Yadav, Y. Singh, A. Kumar, B. Govind, U. Deshpande, S. Hausale, V.N. Singh, Thickness dependent P-N Switching in $SnSe_2/SnO_x/SnSe$ Heterojunction-based NO_2 Gas Sensor as Well as Photodetector, Journal of Science: Advanced Materials and Devices, Vol. 8, 2023, pp. 100583. https//doi.org/10.1016/j.jsamd.2023.100583.

[3] R. Alrammouz, M. Lazerges, J. Pironon, I. Bin Taher, A. Randi, Y. Halfaya, S. Gautier, V_2O_5 Gas Sensors: A Review, Sensors Actuators A Physical, Vol. 332, 2021, pp. 113179, https//doi.org/10.1016/j.sna.2021.113179.

[4] T. T. Nguyet, L. V. Duy, N. C. Nam, D. Q. Dat, H. Nguyen, C. M. Hung, N. V. Duy, N. D. Hoa, Transition from P-type yo N-type Semiconductor in V_2O_5 Nanowire-Based Gas Sensors: Synthesis and Understanding of the Sensing Mechanism, Sensors Actuators B Chemical, Vol. 424, 2025, pp. 136841, https//doi.org/10.1016/j.snb.2024.136841.

[5] N. X. Thai, N. V. Duy, N. V. Toan, C. M. Hung, N. V. Hieu, N. D. Hoa, Effective Monitoring and Classification of Hydrogen and Ammonia Gases with a Bilayer Pt/Sno_2 Thin Film Sensor, International Journal of Hydrogen Energy, Vol. 45, 2020, pp. 2418-2428, https//doi.org/10.1016/j.ijhydene.2019.11.072.

[6] A. Imash, G. Smagulova, B. Kaidar, A. Keneshbekova, R. Kazhdanbekov, L. F. Velasco, Z. Mansurov, Chemoresistive Gas Sensors Based on Electrospun 1D Nanostructures: Synergizing Morphology and Performance Optimization, Sensors, Vol. 24, No. 21, 2024, pp. 6797, https//doi.org/10.3390/s24216797.

[7] E. Afsharmanesh, H. Haratizadeh, F. Bagheri, Self-powered, Highly Selective and Fast Response Time Ammonia Gas Sensors Based on an rGO/SnO_2 Nanocomposite, Sensors Actuators A Physical, Vol. 379, 2024, pp. 115963, https//doi.org/10.1016/j.sna.2024.115963.

[8] Z. Li, W. Zeng, Q. Li, SnO_2 as a Gas Sensor in Detection of Volatile Organic Compounds: A review, Sensors Actuators A Physical, Vol. 346, 2022, pp. 113845, https//doi.org/10.1016/j.sna.2022.113845.

[9] V. Janakiraman, V. Tamilnayagam, R. S. Sundararajan, S. Suresh, C. S. Biju, Structural and Optical Properties of Pure SnO_2 and V_2O_5/SnO_2 Nanocomposite Thin Filmsbfor Gas Sensing Application, Journal of Materials Science: Materials in Electronics, Vol. 31, 2020, pp. 15477-15488, https//doi.org/10.1007/s10854-020-04110-2.

[10] W. C. Ko, K. M. Kim, Y. J. Kwon, H. Choi, J. K. Park, Y. K. Jeong, ALD-assisted Synthesis of V_2O_5 Nanoislands on SnO_2 Nanowires for Improving NO_2 Sensing Performance, Applied Surface Science, Vol. 509, 2020, pp. 144821, https//doi.org/10.1016/j.apsusc.2019.144821.

[11] F. Zhang, X. Wang, J. Dong, N. Qin, J. Xu, Selective BTEX sensor based on a SnO_2/V_2O_5 composite, Sensors Actuators B Chemical, Vol. 186, 2013, pp. 126-131, https//doi.org/10.1016/j.snb.2013.05.086.

[12] L. Van Duy, T. T. Nguyet, D. T. T. Le, N. V. Duy, H. Nguyen, F. Biasioli, M. Tonezzer, C. D. Natale, N. D. Hoa, Room Temperature Ammonia Gas Sensor Based on p-Type-like V_2O_5 Nanosheets Towards Food Spoilage Monitoring, Nanomaterials, Vol. 13, Issue 1, 2023, pp. 146, pp. 1-18, https//doi.org/0.3390/nano13010146.

[13] D. H. Yen, L. Tran, N. Phu, D. Thi, T. Le, Synthesis of Tungsten Oxide Nanofibers Using Electrospinning Towards Gas Sensor Application, Vol. 41, No. 2, 2025, pp. 84-91, https//doi.org/10.25073/2588-1124/vnumap.4993.